VTT Technical Research Centre of Finland

Inversion of True Leaf Reflectance from Very High Spatial Resolution Hyperspectral Images

Ihalainen, Olli; Mõttus, Matti; Juola, Jussi

Published in:
IGARSS 2023 - 2023 IEEE International Geoscience and Remote Sensing Symposium

DOI:
10.1109/IGARSS52108.2023.10283065

Published: 01/01/2023

Document Version
Early version, also known as pre-print

INVERSION OF TRUE LEAF REFLECTANCE FROM VERY HIGH SPATIAL RESOLUTION HYPERSPECTRAL IMAGES

Olli Ihalainen, Matti Mõttus*

VTT Technical Research Centre of Finland
Espoo, Finland

Jussi Juola

Aalto University
Department of Built Environment
Espoo, Finland

ABSTRACT

The spectral reflectance of vegetation obtained from optical sensors provides information on their biophysical and biochemical properties. However, in remote sensing, reflectance is typically computed with respect to the top-of-canopy (TOC) surface, resulting in an apparent reflectance due to the differences between the illumination conditions between the observed vegetation elements and the TOC surface. While the TOC reflectance is useful for data with coarse spatial resolution, it leads to erroneous estimates of the vegetation properties when applied to very high spatial resolution (VHR) data where individual leaves are visible. An illumination correction is required to retrieve the true leaf reflectance from the TOC reflectance. The present work investigates an illumination correction method for retrieving the true leaf reflectance from VHR hyperspectral TOC reflectance images based on the spectral invariant theory and a simple mathematical model for the leaf reflectance. The method is tested on simulated and measured data. The results show that the leaf reflectance can be accurately estimated from both data (average RMSD between 0.02 and < 0.12).

Index Terms— hyperspectral, imaging spectroscopy, reflectance, p-theory, spectral invariant, inversion, radiative transfer

1. INTRODUCTION

The spectral reflectance of vegetation obtained from optical sensors enables the retrieval of their biophysical and biochemical properties. The hemispherical-directional reflectance factor (hereafter called reflectance unless otherwise specified) in a pixel corresponding to a vegetation canopy element such as a leaf or a tree crown is calculated as the ratio of radiance reflected by the canopy element towards the sensor to the theoretical radiance reflected by a reference surface under identical illumination and observation geometry. However, in practice, the latter is commonly calculated using the known spectrum of solar radiation and radiative transfer in the atmosphere or taken from the reflectance of a reference panel next to the vegetated area. Therefore, the reflectance of a pixel is not calculated using the irradiance conditions for the element in the pixel but using that on a top-of-canopy (TOC) surface.

For spectral data recorded by traditional environmental satellites with a medium spatial resolution larger than 10 m, this approach produces reasonable results: reflectance factors for a vegetation canopy. For images with a very high spatial resolution taken from aircraft and drones, where the pixel size is below 1 m, the approach becomes less justified: at such scales, individual canopy elements such as leaves become visible. The illumination conditions on the canopy elements can be considerably different from those at the TOC [1, 2]. Hence, the reflectance calculated for a pixel with respect to the TOC surface does not represent the true reflectance of the canopy element in a pixel.

Previous research has shown that the local illumination conditions for vegetation elements can be accounted for by the spectral invariant theory [3]. Indeed, the spectral invariant theory links the TOC reflectance to the true leaf reflectance via wavelength-independent parameters, which are directly related to the illumination conditions, namely the direct solar irradiance and diffuse ambient irradiance [4]. Recently, [5] demonstrated accurate retrieval of the true leaf reflectance from VHR hyperspectral images using the spectral invariant theory and the PROSPECT-D leaf radiative transfer model [6]. However, PROSPECT is ill-suited for this illumination correction method, as it models the leaf directional-hemispherical reflectance rather than the hemispherical-directional reflectance. Thus, an alternative model for the leaf reflectance is needed.

The main objective of this work was to investigate using a sigmoid function as a leaf reflectance model in the red edge wavelengths (710 to 790 nm) when performing illumination correction on TOC reflectance with the spectral invariant theory. The method enables the retrieval of the true leaf reflectance for visual to near-infrared wavelengths using the spectral invariants retrieved from the red edge.

*Olli Ihalainen is the corresponding author. Email: olli.ihalainen@vtt.fi.

2. MATERIALS

2.1. Simulated data

We used eight synthetic hyperspectral TOC reflectance images by [5], where the true leaf reflectance of each pixel is known a priori. The data were generated using Monte Carlo ray tracing with cyclic boundary conditions such that the simulated vegetation scenes had identical geometric properties but varying leaf optical properties. More specifically, each scene had of a non-reflecting forest floor and 138 randomly positioned and oriented disk-shaped identical bi-Lambertian leaves with a 0.15 m radius within a 1 m $\times$ 1 m area. The ANGERS database was used for the leaf spectra [6]. For one half of the scenes, the reflectance and transmittance factors of leaves 74, 126, 202, and 245 of the ANGERS database were used (Fig. 1a–d). For the other half of the scenes, the corresponding biochemical traits of the leaves from the ANGERS database were used as input for the PROSPECT-D model to generate the leaf spectra (Fig. 1e–h). The simulated wavelengths ranged from 450 nm to 900 nm at 5 nm intervals and the spatial resolution was 1 cm resulting in images with 100 rows and 100 columns.

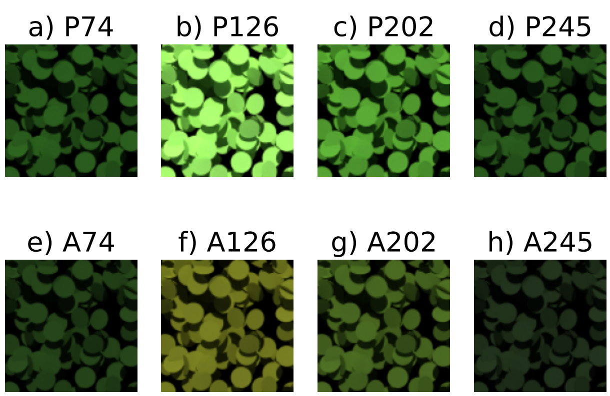

Fig. 1. RGB images of the simulated data scenes. Each leaf in a given scene has the same optical properties.

2.2. Measured data

For the measured data, we used a hyperspectral image of a *Diervilla lonicera* Mill. canopy located in the Otaniemi campus, Finland ($60°11'$ N, $24°49'$ E) by [5]. The image was recorded using a Specim IQ imaging spectrometer (serial number 190-1100152, Specim, Oulu, Finland; 512×512 pixels, spectral resolution 7 nm) from a nadir view geometry on a cloudless day with the Sun at a 47° zenith angle. The instrument was placed approx. 1 m above the canopy, resulting in a spatial resolution of approx. 1 mm. The image was calibrated to TOC reflectance using Spectralon white diffuse reflectance standard (99%) panel placed above the canopy such that it was visible in one corner of the image. The reference reflectance spectra of two sunlit leaves visible in the image were collected using an Avantes SensLine spectometer (AvaSpec-ULS-2048x64TEC-EVO, Avantes, Netherlands) with a bare fiber optic cable in a cross-plane geometry at 45° view zenith angle. As with the simulated data, the wavelengths between 450 nm and 900 nm were selected.

3. THEORY

Let us consider a measurement of the radiance I_s scattered by a sunlit leaf within a vegetation canopy toward the instantaneous field of vision of a sensor above the canopy. The hemispherical-directional reflectance factor of the leaf is given by $R_{\text{leaf}} = \pi I_s/\phi$, where ϕ is the incident irradiance on the leaf [7]. Similarly, the TOC reflectance of the leaf is given by $R_{\text{TOC}} = \pi I_s/\Phi_{\text{TOC}}$, where Φ_{TOC} is the irradiance on the TOC from the above. By decomposing the irradiance on the leaf into direct solar irradiance, $\phi_{\odot}$, and diffuse irradiance from the sky and from within the canopy, ϕ_A, the TOC reflectance can be written as

$$R_{\text{TOC}}(\lambda) = \left[\frac{\phi_{\odot}(\lambda)}{\Phi_{\text{TOC}}(\lambda)} + \frac{\phi_A(\lambda)}{\Phi_{\text{TOC}}(\lambda)}\right] R_{\text{leaf}}(\lambda) \tag{1}$$

$$= \left[\rho + pR_{\text{TOC}}(\lambda)\right] R_{\text{leaf}}(\lambda), \tag{2}$$

where $\frac{\phi_{\odot}}{\Phi_{\text{TOC}}} = \rho$ and $\frac{\phi_A}{\Phi_{\text{TOC}}} = pR_{\text{TOC}}$, and ρ and p are independent of the wavelength [1, 3, 4]. Assuming the leaf reflectance can be parameterized by a vector $\vec{\vartheta}_{\text{leaf}}$ and rearranging Eq. (2), we get a forward model for the TOC reflectance

$$R^{\text{mod}}_{\text{TOC}}(\vec{\vartheta}_{\text{TOC}}; \lambda) = \frac{\rho R^{\text{mod}}_{\text{leaf}}(\vec{\vartheta}_{\text{leaf}}; \lambda)}{1 - pR^{\text{mod}}_{\text{leaf}}(\vec{\vartheta}_{\text{leaf}}; \lambda)} + \varepsilon, \tag{3}$$

where $\vec{\vartheta}_{\text{TOC}} = [p, \rho, \vec{\vartheta}_{\text{leaf}}]^T$ is the model input vector and ε is the measurement and model uncertainty. The present work uses a sigmoid function with three input parameters for modeling the leaf reflectance in the red edge wavelength region (710 to 790 nm)

$$R^{\text{mod}}_{\text{leaf}}(\vec{\vartheta}_{\text{leaf}}; \lambda) = \frac{A}{1 + \exp[k(\lambda - \lambda_0)]}, \tag{4}$$

where A is the upper right asymptote of the logistic curve, k is the logistic growth rate, and λ_0 is the midpoint of the curve. The lower left asymptote of the curve is zero.

4. METHODS

Given the forward model for the TOC reflectance (Eq. (3)), the parameters $\vec{\vartheta}_{\text{TOC}}$ are estimated by minimizing the residual sum of squares between the measured and modeled reflectances in the red edge, $\tilde{\lambda}$

$$\hat{\vec{\vartheta}}_{\text{TOC}} = \text{argmin}_{\vec{\vartheta}_{\text{TOC}}} \sum_{i=0}^{n} \left(R_{\text{TOC}}^{\text{mea}}(\tilde{\lambda}_i) - R_{\text{TOC}}^{\text{mod}}(\vec{\vartheta}_{\text{TOC}}; \tilde{\lambda}_i) \right)^2 , \quad (5)$$

where n is the number of measured wavelengths. The parameter inversion (Eq. 5) was performed using the trust region reflective algorithm implemented in the SciPy library of Python. The initial guess values and the lower and upper bounds of $\vec{\vartheta}_{\text{TOC}}$ are given in Table 1.

Table 1. The initial guess values and upper and lower boundaries of parameters used in the inversion.

	p	ρ	A	k	λ_0
initial guess	0.50	0.90	0.45	0.10	715.00
lower bound	$-\infty$	$-\infty$	0.1	0.00	670.00
upper bound	∞	∞	1.00	0.2	790.00

Given the estimated values of the spectral invariants, $\hat{p}, \hat{\rho}$, the illumination corrected leaf reflectance can be computed for the entire observed spectral domain of the measured wavelengths, λ, from Eq. (2) as

$$R_{\text{leaf}}(\lambda) = \frac{R_{\text{TOC}}(\lambda)}{\hat{\rho} + \hat{p} R_{\text{TOC}}(\lambda)}. \quad (6)$$

The complete illumination correction algorithm thus consists of two steps:

1. Parameter inversion: estimate $\hat{\vec{\vartheta}}_{\text{TOC}} = [\hat{p}, \hat{\rho}, \hat{\vec{\vartheta}}_{\text{leaf}}]^T$ using wavelengths between 710 and 790 nm (Eq. (5)).

2. Illumination correction: compute the true leaf reflectance (Eq. (6)) for all observed wavelengths using $\hat{p}, \hat{\rho}$.

5. RESULTS AND DISCUSSION

Overall, the the estimated leaf reflectance spectra produced by the illumination correction algorithm were in good agreement with the true leaf reflectances for both the simulated and measured hyperspectral data. For the simulated images, we computed the RMSD between the estimated and the true leaf reflectances for the sunlit pixels (Fig. 2). Despite a number of outlier values, the mean RMSDs of the scenes were between 0.02 and 0.12, and the standard deviations of the RMSDs were between 0.002 and 0.01. The outliers were caused by pixels where the Monte Carlo simulation noise was high such as pixels between the leaf edges and the black forest floor.

For the measured data (Fig. 3a), the method significantly reduced the effects of illumination conditions of the TOC reflectance for most of the leaves in the image (Fig. 3b). For

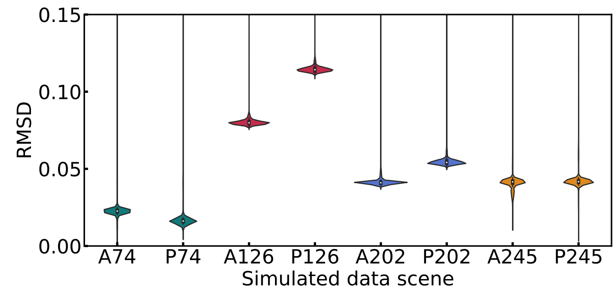

Fig. 2. The distributions of the RMSD values between the estimated leaf reflectances and the true leaf reflectances of the simulated data scenes.

the reference leaf A, the RMSD between the estimated and measured leaf reflectance was 0.02, (Fig. 3c), and for leaf B the RMSD was 0.06 (Fig. 3d).

Although the results from both simulated and measured data were promising, we found that the reflectance produced by the illumination correction algorithm is heavily dependent on the initial guess values for the parameters A and λ_0 of the sigmoid function (Eq. (4)). In fact, the parameter inversion did not generally converge far from the initial values of A and λ_0 (data not shown) meaning that variation in the RMSD values for the data can be partially attributed to how closely the sigmoid function with the initial guess parameters matches the true leaf reflectance at the red edge. E.g., for the scene P74 the sigmoid curve with the initial guess values was already close to the true leaf reflectance, whereas for the scene P126 it was not. The non-uniqueness of the solution for Eq. (5) is a hallmark of ill-posed inverse problems. A unique solution could be sought by imposing a other regularization strategies than setting upper and lower parameter bounds as done in the present work. Alternative approaches are offered by using Bayesian inference, where the unknown parameters are treated as random variables [8], or by training a machine learning method on simulated data for estimating the spectral invariants.

Despite the issues caused by the ill-posedness of the inverse problem, these results can have major implications for hyperspectral vegetation monitoring applications relying on VHR data, e.g., when taken from a unmanned aerial vehicle, which show strong multiple-scattering effects. In this situation, the traditional radiative transfer models used for vegetation (e.g., SAIL [9]) are not applicable, as the vegetation canopy cannot be considered to consist of infinitesimally small scattering elements. The theory of spectral invariants makes no such assumptions and can reduce the effects of the local illumination conditions and scale the measured canopy-level reflectance factor to that of a leaf, enabling detection of the true physiological signals from the canopy elements.

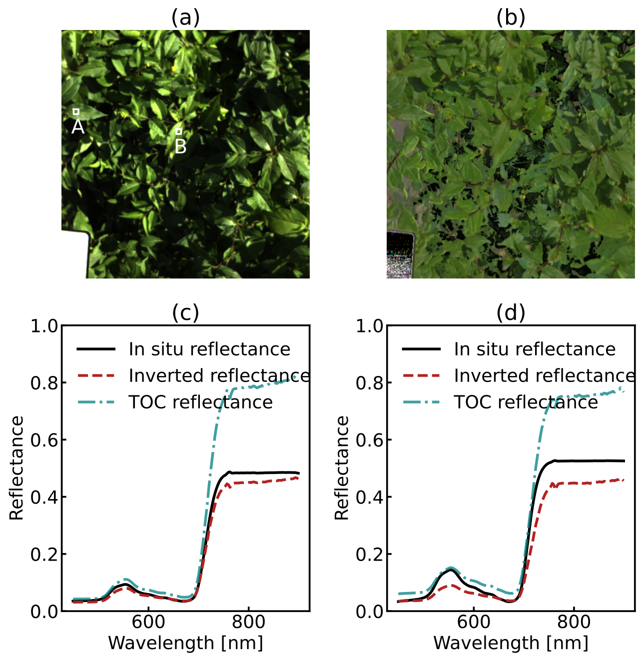

Fig. 3. TOC reflectance image of the *Diervilla lonicera* Mill. canopy with the pixels corresponding to the in situ measured area of leaves A and B shown respectively in cyan and fuchsia (a), an inverted reflectance RGB image (b), the situ measured reflectances and the corresponding averaged TOC and inverted reflectances of leaf A (c) and leaf B (d).

6. CONCLUSION

The present work evaluated the performance of an illumination correction method for retrieving the true reflectance of sunlit leaves from very high spatial resolution hyperspectral TOC reflectance images. The method relates the TOC reflectance to the true leaf reflectance via the spectral invariant theory and uses a sigmoid function to model the leaf reflectance. The results show that the method can accurately retrieve the leaf reflectance under varying illumination conditions. The illumination corrected true leaf reflectance spectrum enables the accurate estimation of leaf biochemical variables, such as leaf chlorophyll content. However, the results depend heavily on the initial guess values for the parameters inverted by the method. Hence, further research is should focus on increasing the robustness of the method.

7. ACKNOWLEDGMENTS

This work was funded by the Academy of Finland (grant 322256).

8. REFERENCES

[1] Matti Mõttus, Tuure L.H. Takala, Pauline Stenberg, Yuri Knyazikhin, Bin Yang, and Tiit Nilson, "Diffuse sky radiation influences the relationship between canopy PRI and shadow fraction," *ISPRS Journal of Photogrammetry and Remote Sensing*, vol. 105, pp. 54–60, 7 2015.

[2] Forrest G Hall, Thomas Hilker, Nicholas C Coops, Alexei Lyapustin, Karl F Huemmrich, Elizabeth Middleton, Hank Margolis, Guillaume Drolet, and T Andrew Black, "Multi-angle remote sensing of forest light use efficiency by observing PRI variation with canopy shadow fraction," *Remote Sensing of Environment*, vol. 112, no. 7, pp. 3201–3211, 2008.

[3] Rocio Hernandez-Clemente, Pasi Kolari, Albert Porcar-Castell, Lauri Korhonen, and Matti Mõttus, "Tracking the Seasonal Dynamics of Boreal Forest Photosynthesis Using EO-1 Hyperion Reflectance: Sensitivity to Structural and Illumination Effects," *IEEE Transactions on Geoscience and Remote Sensing*, vol. 54, no. 9, pp. 5105–5116, 9 2016.

[4] Olli Ihalainen and Matti Mõttus, "Spectral invariants in ultra-high spatial resolution hyperspectral images," *Journal of Quantitative Spectroscopy and Radiative Transfer*, p. 108265, 2022.

[5] Olli Ihalainen, Jussi Juola, and Matti Mõttus, "Physically based illumination correction for sub-centimeter spatial resolution hyperspectral data," unpublished.

[6] Jean-Baptiste Feret, Christophe François, Gregory P Asner, Anatoly A Gitelson, Roberta E Martin, Luc PR Bidel, Susan L Ustin, Guerric Le Maire, and Stéphane Jacquemoud, "PROSPECT-4 and 5: Advances in the leaf optical properties model separating photosynthetic pigments," *Remote sensing of environment*, vol. 112, no. 6, pp. 3030–3043, 2008.

[7] G. Schaepman Strub, M. E. Schaepman, T. H. Painter, S. Dangel, and J. V. Martonchik, "Reflectance quantities in optical remote sensing-definitions and case studies," *Remote Sensing of Environment*, vol. 103, no. 1, pp. 27–42, 7 2006.

[8] Daniel Schraik, Petri Varvia, Lauri Korhonen, and Miina Rautiainen, "Bayesian inversion of a forest reflectance model using sentinel-2 and landsat 8 satellite images," *Journal of Quantitative Spectroscopy and Radiative Transfer*, vol. 233, pp. 1–12, 2019.

[9] Wouter Verhoef, "Light scattering by leaf layers with application to canopy reflectance modeling: The SAIL model," *Remote sensing of environment*, vol. 16, no. 2, pp. 125–141, 1984.